Structure Function Analysis of Blazars AP Librae and 3c279

Anders A. Jensen
Adviser: Dr. Robert Knop
Vanderbilt University
Department of Physics and Astronomy

April 27, 2008

Abstract

Blazars AP Librae and 3c279 are analyzed for microvariability using a technique known as structure function analysis. AP Librae was observed in April of 2005 and 3c279 was observed in April of 2007. The data for AP Librae was previously reduced by Andrew Collazzi and the author reduced the data for 3c279. Both sets of data were reduced using Robert Knop's data reduction program.

The author ran structure function analysis on both sets of data. Structure function analysis is a statistical analysis run on data that is suppose to find timescales of variability, periodicity, and the noise type of data. Previous analysis of AP Librae confirmed mircrovariability, which also shows up in the structure function of AP Librae. Blazar 3c279 was much quieter than AP Librae and showed no microvariability durning any of the nights.

Contents

1 Active Galactic Nuclei **1**
1.1 Introduction 1
1.2 Microvariability 1

2 Data Reduction **3**
2.1 Introduction 3
2.2 CCD Chips 3
2.3 Overscan 4
2.4 Zero Subtraction 4
2.5 Flatfields 5

3 Lightcurves **6**
3.1 Introduction 6
3.2 Comparison Stars 6

4 Structure Function Analysis **8**
4.1 Introduction 8
4.2 White, Flicker, and Shot Noise 8
4.3 Characteristic Timescales and Periodicity 9
4.4 Created Lightcurves 10

5 Results **19**
5.1 3c279 19
5.2 AP Librae 25

6 Conclusions **29**
6.1 Microvariability 29
6.2 Structure Functions 29
6.3 Future Goals 29

7 Acknowledgments & References **30**

1 Active Galactic Nuclei

1.1 Introduction

Active galactic nuclei (AGNs) are a class of galaxy with an active center that is most likely powered by accretion into a black hole. AGNs can have large relativistic jets that extend out hundreds of thousands to millions of light years.

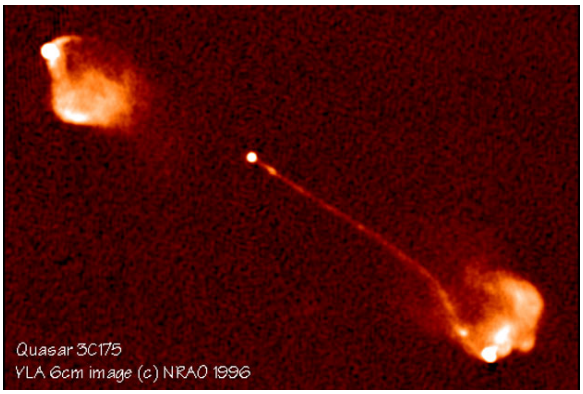

Figure 1.1: *The above picture shows a radio image of 3c175 which is an AGN with relativistic jets. (http://antwrp.gsfc.nasa.gov/apod/image/0109/3c175_vla_big.gif)*

AGNs are known for their small angular size and a bright luminosity. AGNs can have a luminosity of 10^{48} *ergs/s* in much less than 1 pc^3 while a field galaxy typically has a luminosity of 10^{44} *ergs/s* (Krolik, 1999). AGNs are known as flat-spectrum objects and about one third of flat-spectrum objects (see fig. 1.2) show rapid variability on timescales of less than two days (Kraus et al. 1999).

There is a strong peak in AGN active at a redshift of $z = 2$ which is when most galaxies were young and therefore it is thought that AGNs could possibly shape the way galaxies evolve (Krolik, 1999). Also, a lot of galaxies are thought to have a black hole at their centers which are not active, but may have at one point been active. Understanding how AGNs shape galaxies and trying to understand if all galaxies go through an AGN phase at some point in time are the bigger picture concepts that envelop the study of blazar microvariability.

Blazars are a class of Active galaxy that combine BL Lacertae and OVV (optically violently variable) objects (Krolik, 1999). The jets of a blazar are pointed towards the line of sight of Earth meaning that we can observe down the jet of the blazar. Blazars exhibit a characteristic known as microvariability. Microvariability is the variability of brightness on time scales of less than a day, but blazars are also known to vary on larger time scales likes weeks and years. Also, blazars are known to vary in all parts of the electromagnetic spectrum (Stalin et al. 2006). In the optical band, variability of 0.13 magnitudes has been detected on timescales as short as 720 seconds (Ghosh et al. 2000).

1.2 Microvariability

Studying blazar microvariability has led to two main different conclusions on the source of microvariability. Some theories promote the idea that microvariability is intrinsic to the source, while other theories say that microvariability is caused by

extrinsic means. If microvariability is intrinsic to the source, then an upper limit on the size of the emitting region of the source can be calculated (Wagner & Witzel, 1995). This upper limit is $R < c \cdot \Delta t$ where R is the size of the emitting region, c is the speed of light and Δt is timescale of variability. One of the main extrinsic theories states that instabilities in the accretion disk (see fig. 1.3) produce the microvariability (Wiita, 1996). Another extrinsic theory involves interstellar scintillation (ISS) which results from density inhomogeneities of the interstellar medium (ISM). These inhomogeneities are thought to cause diffractive and refractive scattering which leads to variability (Wagner & Witzel, 1995). When comparing variability in both the radio and optical bands, close correlation between the two suggests that variability is most likely intrinsic. Also, while ISS could cause variability in the radio band, it is unlikely that it causes variability in the optical band. The leading theory for intrinsic variability proposes that shocks in the relativistic jets of AGNs cause variability. These jets which consist of a plasma with very high conductivity, are collimated by strong and twisting magnetic field lines. Particles that encounter theses shocks along with the twisting magnetic field lines will emit synchrotron radiation (Meier et al. 2001).

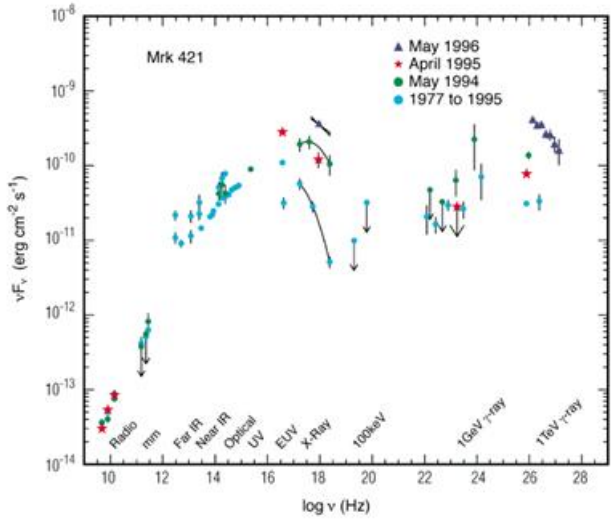

Figure 1.2: *The spectrum of BL Lac object Mrk 421. Most AGN have a relatively flat spectrum as compared to normal galaxies. Notice how the spectrum of Mrk 421 stays relatively flat from IR to gamma rays. (http://heasarc.gsfc.nasa.gov/docs/cgro/images/epo/gallery/agns/agn_spectra.gif)*

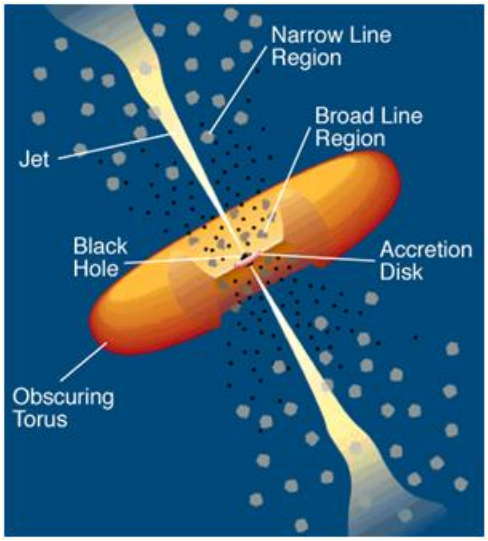

Figure 1.3: *A cartoon image of an AGN. Accretion into a black hole is thought to power the jets. The jets are collimated by magnetic field lines. (http://heasarc.gsfc.nasa.gov/docs/cgro/images/epo/gallery/agns/agn_up_model.gif)*

2 Data Reduction

2.1 Introduction

The data used were taken from the Cerro Tololo Inter-American Observatory (CTIO) in Chile in April of 2005 and April of 2007. The images of AP Librae were from 2005 and those data were previously reduced by Andrew Collazzi and is included in his thesis titled *Microvariability in AP Librae and PKS 1216-010*. The images of AP Librae were 120 second exposures in both R and B filters. These images were taken with the 1.0 meter telescope at CTIO. AP Librae was observed with both R and B filters for two nights for about 5.5 hours per night. The author performed structure function analysis on the AP Librae data. The images of 3c279 were from 2007 and the author reduced that data and ran structure function analysis on it. The images of 3c279 were 60 second exposures using an R filter. 3c279 was observed over 4 nights for about 7 hours per night. These images were taken with the 0.9 meter telescope at CTIO.

Object	RA	DEC
AP Librae	15h 17m 41.8s	-24d 22m 19s
3c279	12h 56m 11.1s	-05d 47m 22s

Table 1: *Positions of the objects used from NASA/IPAC Extragalactic Database (NED) (http://nedwww.ipac.caltech.edu/)*

2.2 CCD Chips

CCD chips are an array of pixels that store the images. As photons from blazars and other bright objects in the night sky hit the chip, the different pixels count

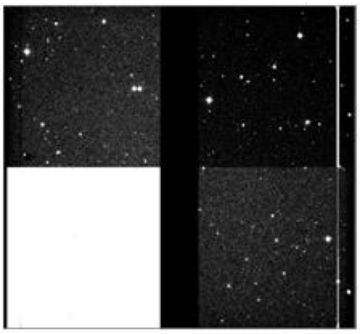

Figure 2.1: *An image of raw data.*

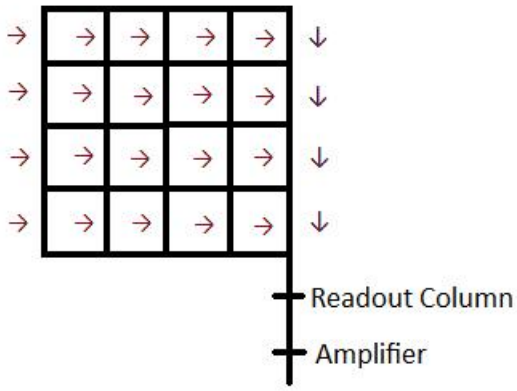

Figure 2.2: *A diagram of pixel readout.*

the number of photons and different values refer to different shades from black to white. When a photon hits a pixel, a photoelectron is released and captured in a potential well. The more photons that are detected by a pixel, the whiter the pixel will appear in the final image. The pixels are read into a computer one at a time where the charge stored in each pixel from the captured photoelectrons is shifted down into the readout column and then into an amplifier. After the charge stored in every pixel is read in a column, all the columns shift so another column can be read out. Figure 2.2 shows how a CCD chip with 16 pixels would be read into a computer. Each box represents a pixel and the arrows show how the pixels are read out. After all the pixels are read out, a few more columns with no stored data are sent to the readout column which leads to the overscan region. The overscan region is in the image, but is not part of the image and needs to be removed.

2.3 Overscan

The first step in data reduction is removing the overscan region. The overscan region for the data was located in the middle of the image (seen in figure 2.1 as the black strip down the middle) and is a result of counting extra columns of pixels after all the data has been counted. The overscan region is therefore the result of sending empty pixels through the amplifier and is useful in measuring the amplifier bias. The raw data had four different regions because the pixels were counted four at a time in order to increase the speed at which the data could be read and stored. The four regions look different because they are read out through four different amplifiers. Because the pixels were read out four at a time, the raw data had four overscan regions which are boxed in blue in figure 2.3. The overscan regions were removed because they are not actually a part of the image.

2.4 Zero Subtraction

The next part of data reduction is zero subtraction. Zero subtraction removes pixel to pixel variations that are intrinsic to the pixels. Zero images are images with no exposure time and are therefore just blank images. One zero image was built from combining many zero images and this zero was subtracted from all the images. This

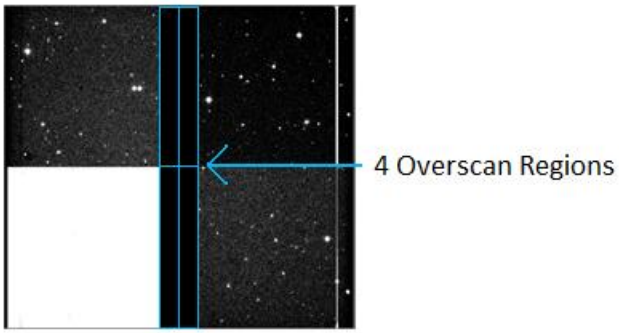

Figure 2.3: *Raw data with the four overscan regions highlighted.*

means that every pixel value in the zero image is subtracted from the corresponding pixel value in the data.

2.5 Flatfields

Flatfield corrections are used because different pixels react differently when exposed to light. There are two different types of flatfield images that Professor Knop took. Dome flats are images of an out of focus light source. Sky flats are images of the sky during twilight. Sky flats were used for the flatfield correction because the sky flats were better. The sky flats were combined for one night to create a sky flat by which my data was divided. The purpose of a flatfield correction ensures that errors arising from different pixel efficiencies are removed. Flatfield images are images where every pixel is equally illuminated by a light source (such as the twilight sky in our case) and so discrepancies in photon count can be seen and removed from actual data. The flatfield was divided out of the data which means that every pixel in the data was divided by the corresponding pixel in the flatfield.

3 Lightcurves

3.1 Introduction

After my data was reduced I produced lightcurves for my data. A lightcurve shows the differential magnitude of an object versus time which is usually in Julian date. Julian data (JD) is just the number of days that have passed since noon on January 1, 4714 BC.

Lightcuves are usefully because they show how an object changes brightness over time. In the study of blazar microvariability, variability is studied on very short time scales. As seen in figure 3.1, AP Librae changes 0.3 magnitudes from 2453466.77 to 2453466.82 which is a significant magnitude change in approximately 0.05 JD which is 0.05 days or about 1.2 hours. The data reduction and production of lightcurves for AP Librae was done by Andrew Collazzi (2006).

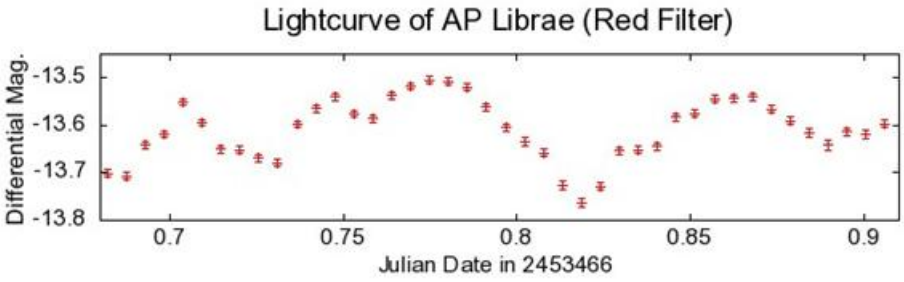

Figure 3.1: *A lightcurve of AP Librae.*

3.2 Comparison Stars

Comparison stars are used to ensure that there is actually variability in the data. If there is variability in a star that is not suppose to vary and that same variability shows up in the blazar then the variability in the blazar cannot be believed. Figure 3.3 shows AP Librae as compared to a comparison star. The comparison stars for 3c279 can be seen in figure 3.4.

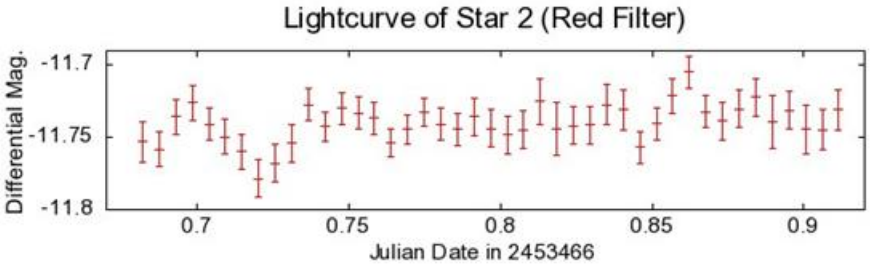

Figure 3.2: *A lightcurve of a comparison star.*

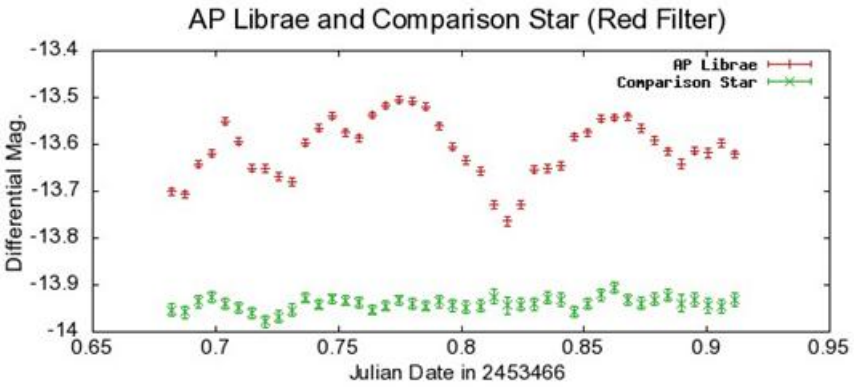

Figure 3.3: *Lightcurve of AP Librae and a comparison star. The magnitude of the comparison star had a constant added to it so it could be compared with AP Librae. This plot shows that the microvariability seen in AP Librae is real.*

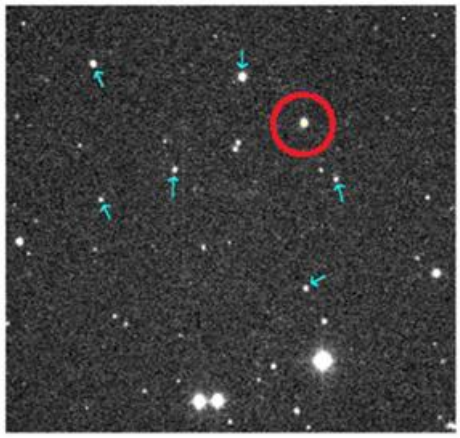

Figure 3.4: *Blazar 3c279 and some comparison stars. The blazar is circled in red and some comparison stars are noted with light blue arrows.*

4 Structure Function Analysis

4.1 Introduction

The structure function (SF) of a lightcurve is used to determine the characteristic time scales of variation in data, and it is also used to determine the periodicity of data. The slope and style of the SF can show important characteristics about the variability of active galactic nuclei. The first order SF as defined by Simonetti et al. (1985) is

$$SF =< [F(t) - F(t + dt)]^2 >$$

where F is flux and t is time. A plot of what a typical SF looks like is shown in figure 4.1.

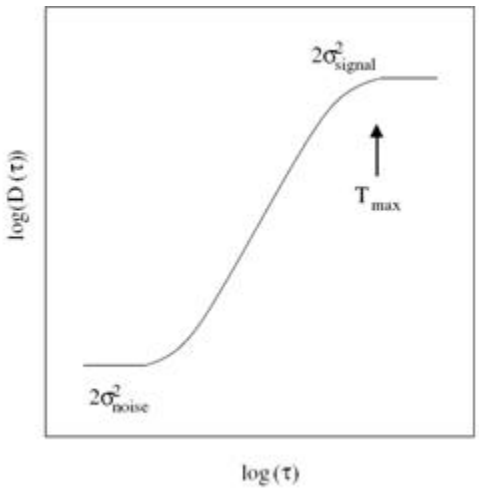

Figure 4.1: *The above image (Hovatta et al. 2007) shows an ideal SF. Note that SFs are usually plotted in a log-log scale.*

Current research studying blazar microvariability leaves a lot of ambiguity in how a SF will look given a lightcurve, so the author did some research and ran SFs on various randomly created lightcurves and line segments with different amounts of shot and flicker noise to attempt to understand SFs better.

4.2 White, Flicker, and Shot Noise

Structure functions show many important characteristics about their respective lightcurves. The initial slope of a SF tells whether the signal is white noise, flicker noise, or shot noise. If data is uncorrelated, it will produce white noise which will have an initial slope of zero on the SF (see fig. 4.2 & fig. 4.3). The data points in a white noise dominated event do not depend on each other (Hufnagel & Bregman 1992). Shot noise shows up on a SF as a slope of 1 and shot noise comes from a sequence of random pulses. Flicker noise is halfway between white noise and shot noise.

Hufnagel & Bregman (1992) define flicker noise as data where the next point depends on the previous data point, but that dependency decreases the further the

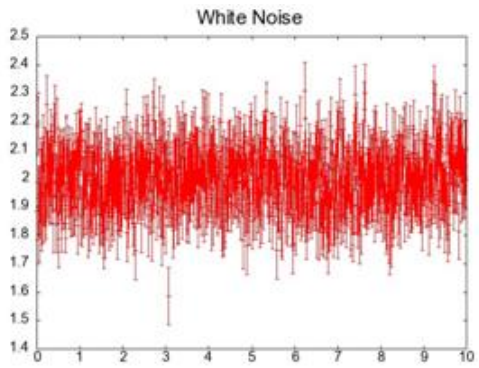

Figure 4.2: *This image shows white noise around a y-value of 2 with a sigma of 0.1.*

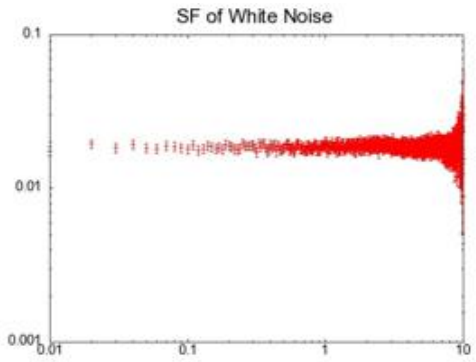

Figure 4.3: *This figure shows the SF of figure 4.2 in the typical log-log scale. White noise shows up with an initial slope of zero on a SF.*

points are away from each other. These authors say that some examples of flicker noise are the number of papers published by scientists and the statistics of the flooding of the Nile. Flicker noise in the radio band is theorized to exist because of refractive interstellar scintillation (RISS). Although variability in the radio and optical bands are usually correlated, there is no evidence that flicker noise in the optical band should be a result of RISS. Theoretical SFs have been built using the mathematics behind RISS and data from the radio band, but it appears that no theoretical work has been done on blazars showing flicker noise in the optical band or on blazars showing shot noise. The theoretical SFs (Blandford et al. 1986) were first order and were based on a particular model for the interstellar medium. Experimental data from Heeschen et al. (1987) agrees very well with the theoretical model from Blandford et al. (1986) and the former authors concluded that the variability in some of their sources (see fig. 4.4) was due to day-to-day flickering caused by RISS.

Shot noise usually shows up as a slope of one in a SF, although if one large outburst dominates the data series then a slope greater than one can exist on a SF (Hovatta et al. 2007). Hugnagel & Bregman (1992) describe shot noise as a set of data points where each point is depended on the other and each point has an infinite memory of the other points. This differs from flicker noise because the dependency each point has on the other points decreases as the points become further away with flicker noise, and therefore the memory of flicker noise is finite. Also, a slope of two can show up in a SF if strong linear or periodic oscillations occur in the data.

4.3 Characteristic Timescales and Periodicity

Another important feature of the SF is that it finds characteristic timescales in data, and it finds periodicity in data. Characteristic timescales show up as a maximum in SFs and periodicity shows up as a minimum. The characteristic timescale is the minimum time interval in which microvariability can be detected. It is not uncommon for a SF to climb to a maximum or fall to a minimum near the end of the SF. If most of the variability occurs from the beginning of the lightcurve to the

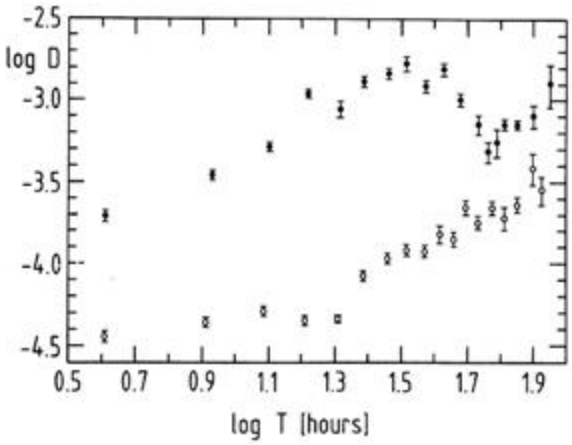

Figure 4.4: *In the above graph (Heeschen et al. 1987), the authors describe the differences between two types of SF that show flicker noise in the radio band. Type I SFs (light circles) shows flicker noise while the type II SFs (dark circles) shows flicker noise with the possibility of mixed shot noise. The type II SF shows more variability. Type I SFs usually do not show a defined maximum (characteristic time scale of variability) while the type II SFs have a maximum. The authors type I SFs are what agreed with the theoretical data from Blandford et al. (1986).*

end with not a lot of variability in the middle, then the characteristic timescale will be detected for the whole lightcurve which will put the maximum of the SF at the end of the SF. If a lightcurve shows periodicity over the entire lightcurve then the SF will fall to a minimum at the end of the SF.

4.4 Created Lightcurves

To better understand SFs, the author ran SFs on different line segments and randomly created lightcurves to observe how different amounts of shot and flicker noise influence SFs. The randomly generated lightcurves were generated with a computer code written by the author. In order to ensure similar amounts of shot and flicker noise, the code was written in the following described manner. An initial magnitude was chosen to correspond with an initial time. All the following points were evenly spaced in time. A second point was chosen to be within a random magnitude of the first point. After these two points were defined, the following points had either a 50 percent chance of being linearly dependent on the previous two points within a random error or a 50 percent chance of being within a random magnitude of only the previous point. This setup ensured an even mix of shot and flicker noise. The lines, which were also created using a computer code are shown in figures 4.5 through 4.8, and the randomly created lightcurves are shown in figures 4.9 through 4.16.

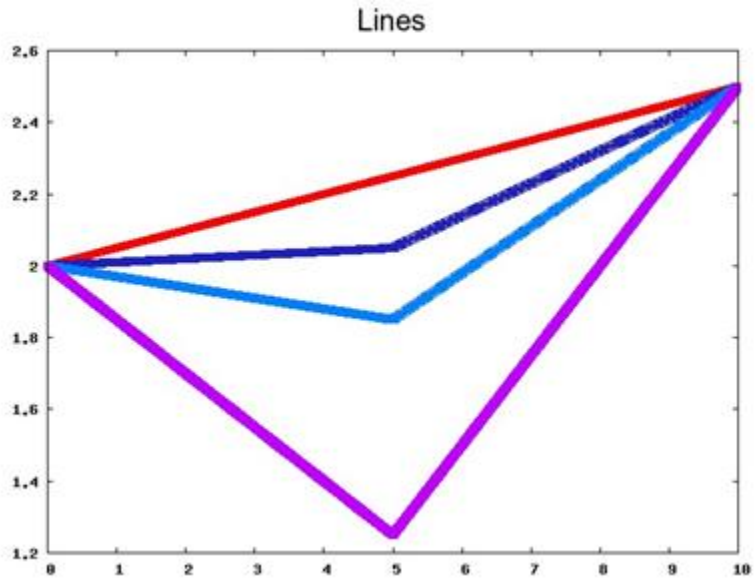

Figure 4.5: *This image shows lines with the same start and end points but with different degrees of bend in the middle.*

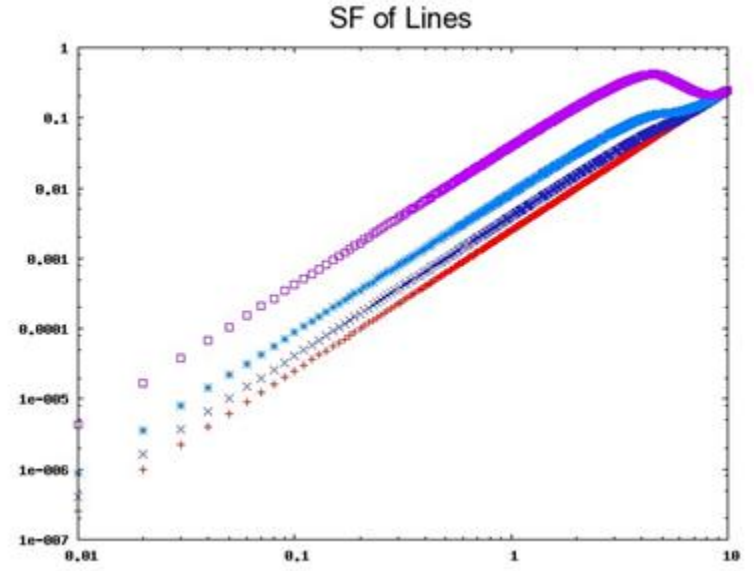

Figure 4.6: *Here we see the corresponding SFs to the lines in figure 4.5 which have increasingly more prominent bends. Notice how a characteristic timescale (maximum) is not recognizable until the bend becomes much larger than the overall slope.*

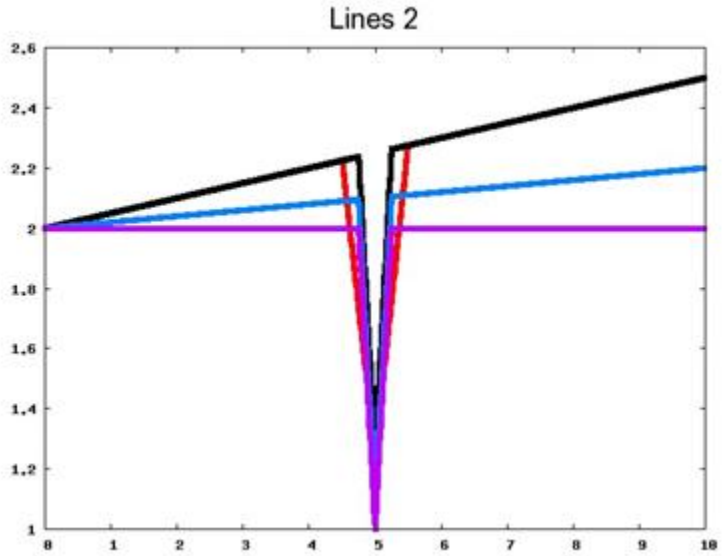

Figure 4.7: *This image shows three lines (black, blue, purple) with the same size spike but different overall slopes. The red line has a bigger spike.*

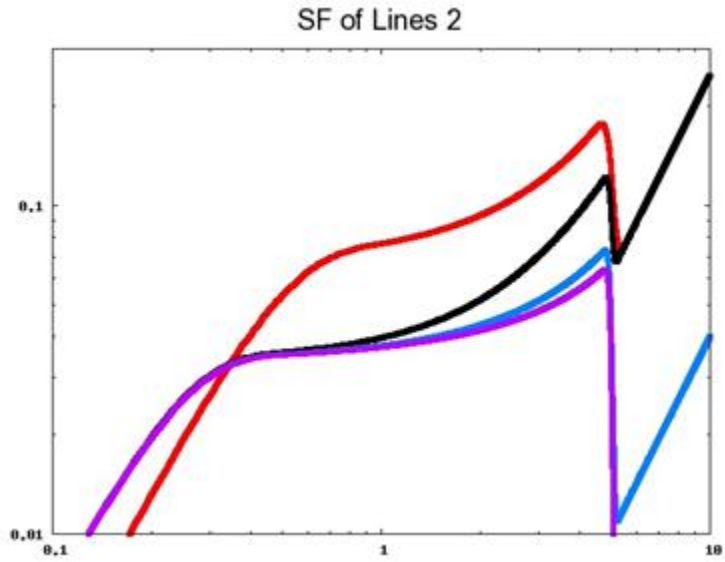

Figure 4.8: *There is a characteristic timescale detected at the interval of where the spike starts to the tip of the spike for each line. This characteristic timescale is 0.25 for the black, blue, and purple lines and 0.5 for the red line and this agrees with the data. There is another characteristic timescale detected for half the entire interval.*

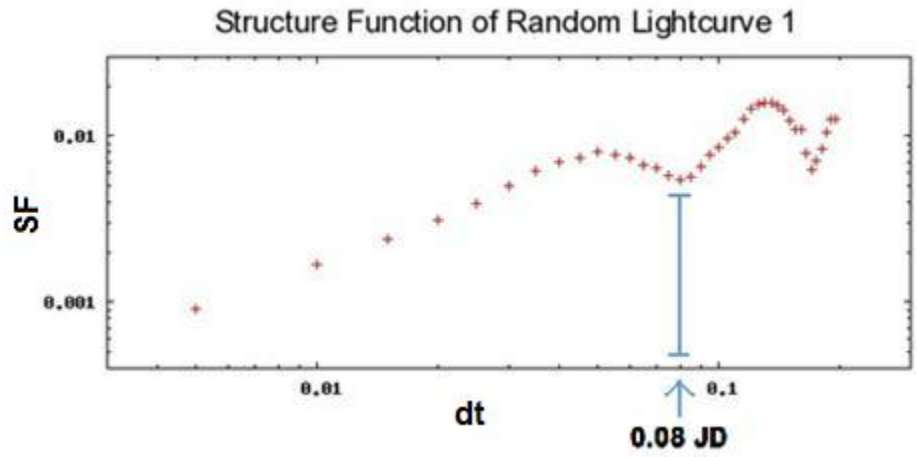

Figure 4.9: *This is the SF for the lightcurve in figure 4.10. The minimum at 0.08 JD means that the lightcurve should be periodic and have a period of 0.08 JD.*

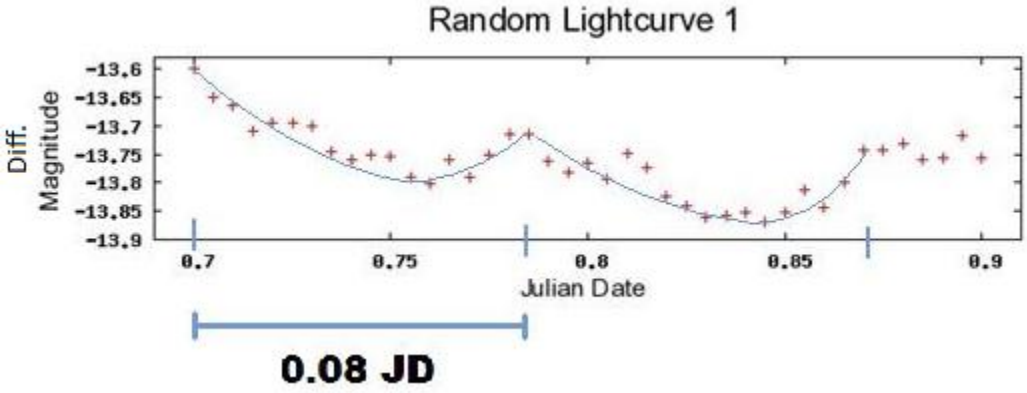

Figure 4.10: *This lightcurve appears to be period with a period of 0.08 JD which is consistent with what its SF shows. However, the periodicity is only apparent because the lightcurve generation code did not have any periodicity written into it.*

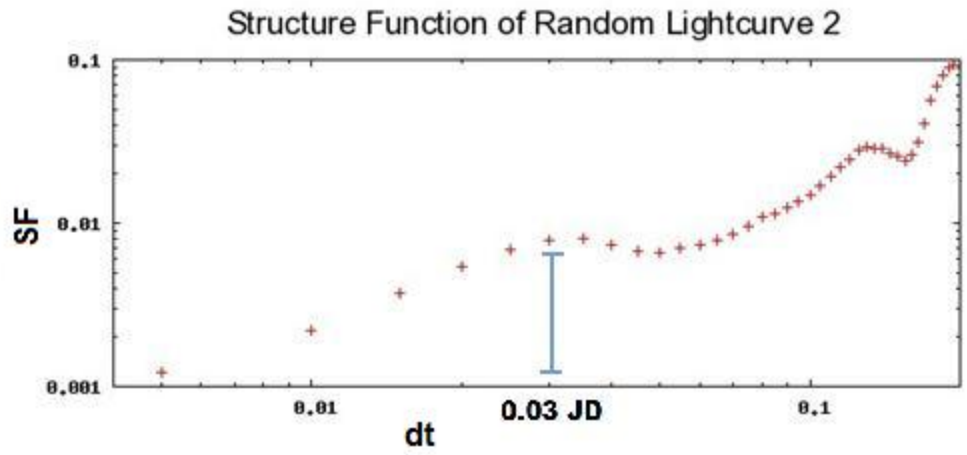

Figure 4.11: *This is the SF for the lightcurve in figure 4.12. The maximum at 0.03 JD means that there should be a characteristic timescale of 0.03 JD.*

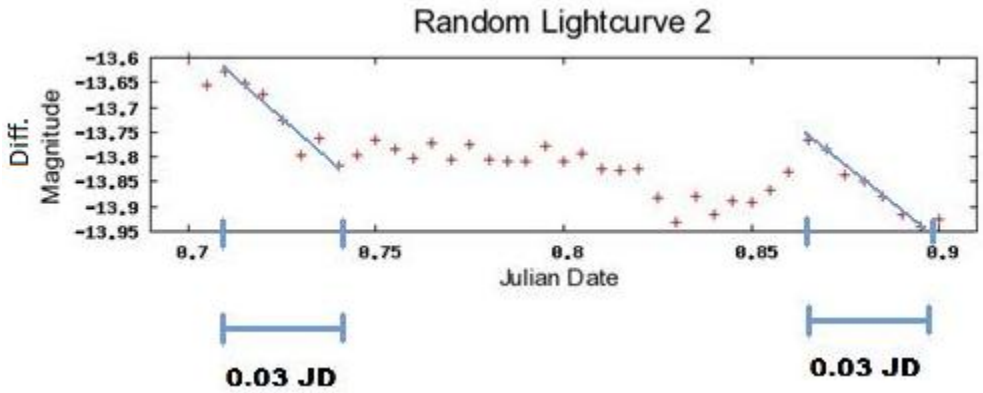

Figure 4.12: *This lightcurve shows a characteristic timescale of 0.03 JD which is consistent with what its SF shows.*

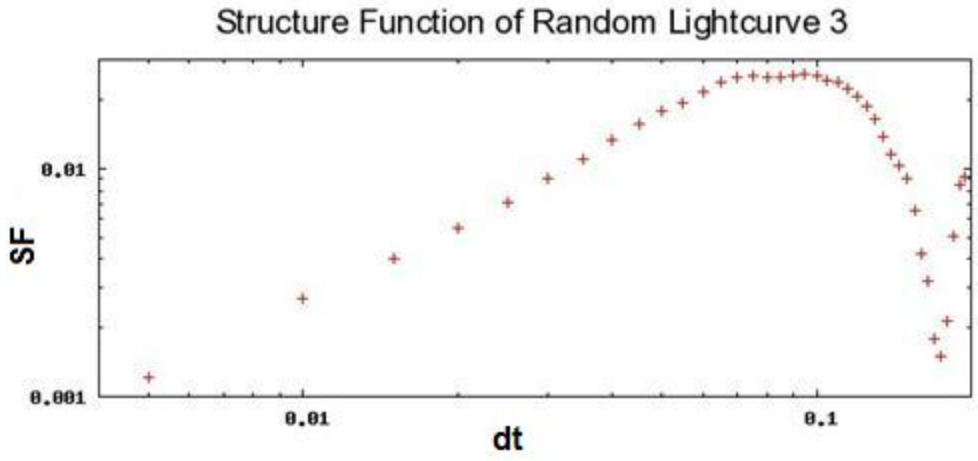

Figure 4.13: *This is the SF for the lightcurve in figure 4.14. This SF falls to a minimum at the end which indicates that the SF is picking up periodicity over the entire lightcurve.*

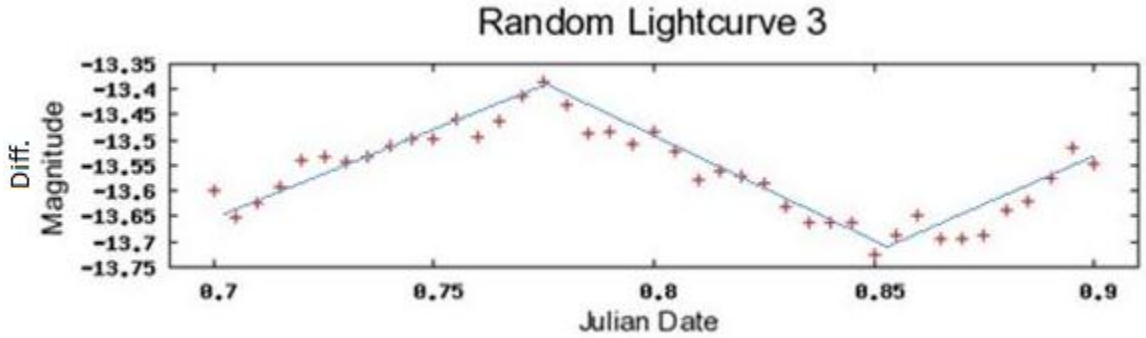

Figure 4.14: *This lightcurve appears to be period over the entire lightcurve which is consistent with what its SF shows. However, the periodicity is only apparent because the lightcurve generation code did not have any periodicity written into it.*

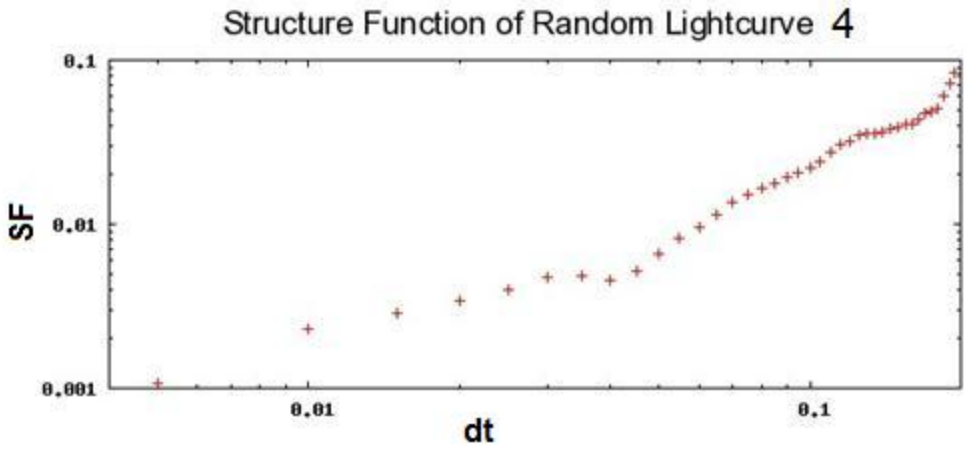

Figure 4.15: *Here the SF climbs to a maximum at the end of the SF which suggests that the lightcurve has a characteristic timescale that lasts the length of the entire lightcurve. In other words, the overall trend of the lightcurve outweighs any smaller variability that is seen. There is a small plateau seen to correspond to a dt of JD = 0.03 which suggests that some variability should be seen on that timescale, but it should be insignificant as compared to the overall trend.*

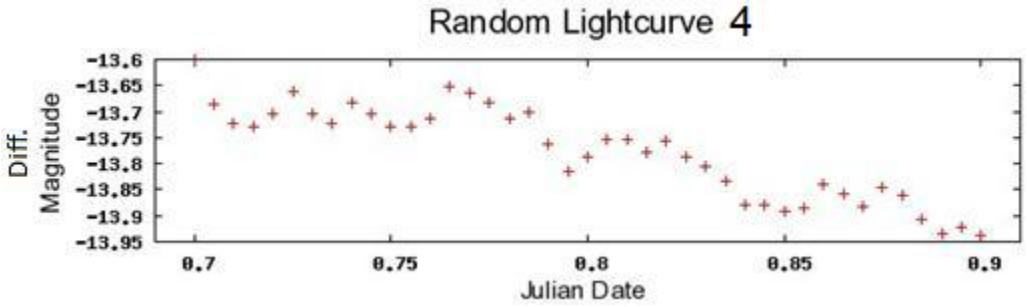

Figure 4.16: *The trend downward that is seen over the entire lightcurve outweighs any microvariability within the lightcurve which is consistent with what the SF shows.*

Figure 4.17 and figure 4.18 (shown on the next page) illustrate some important aspects of SFs. The first lightcurve which is labeled "1" in figure 4.18 and is plotted in red is an original lightcurve of AP Librae. For lightcurve 2, the author took the original lightcurve of AP Librae and changed the magnitude of three points (boxed in red) in order to start removing the flare that is seen to peak at JD 2453466.82. The SFs of the lightcurves are shown in figure 4.17 and each SF is color coordinated with its respective lightcurve. Changing the magnitude of three points in the major flare of the lightcurve does not change the SF much. Removing the entire major flare, which is done in lightcurve 3, changes the SF drastically. The SF corresponding to lightcurve 3 shows a new characteristic timescale at approximately 0.02 JD. This new characteristic timescale is from the small flare that is seen at the beginning of the lightcurve. This analysis proves that the characteristic timescale detected in AP Librae is in fact from the flare that is seen to peak at JD 2453466.82, and that less significant variability can be hidden by more significant variability in SFs. In lightcurve 4, the small flare at the beginning of the lightcurve is partially removed and the characteristic timescale for the most part disappears. In lightcurve 5, the magnitudes of the first two points in the lightcurve are changed which changes the end of the SF; the lightcurve is now more periodic over the entire lightcurve instead of variable. Another important observation is that the slope gradually decreases as the lightcurve of AP Librae is transformed from partially shot dominated to flicker dominated.

Studying SFs has led to a few basic conclusions:

1. Characteristic timescales show up as maximum in SFs.

2. Periodicity shows up as a minimum in SFs.

3. Although SFs can show more than one characteristic timescale of variability, sometimes they show one maximum if there is a dominate flare. Just looking for the maximum in a SF won't necessarily reveal the shortest timescale of significant variation.

4. Data at the end of a SF can sometimes be misleading because at long timescales the SF is greatly influenced by few samples at large separations and by the windowing of the data. This is evident in figure 4.8 where a characteristic timescale appears at half the length of the data set because of the fact that the data set is finite.

5. Periodicity detected at long timescales that come right after characteristic timescales could just be a result of a flare.

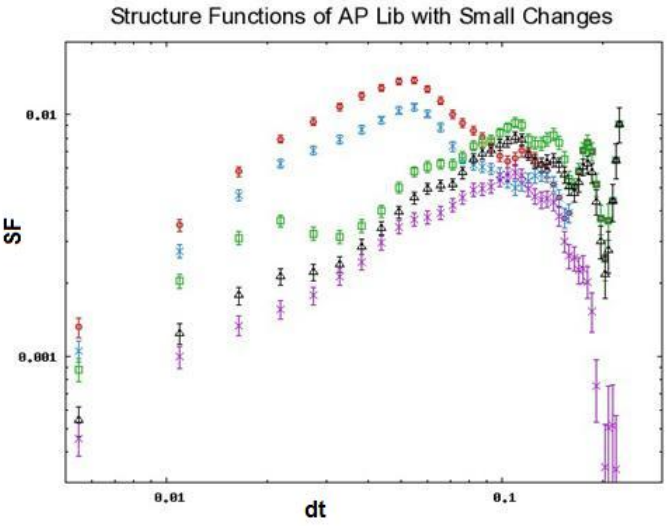

Figure 4.17: *A SF of AP Librae evolving with changes to the lightcurve. See figure 4.18 and the previous text for description.*

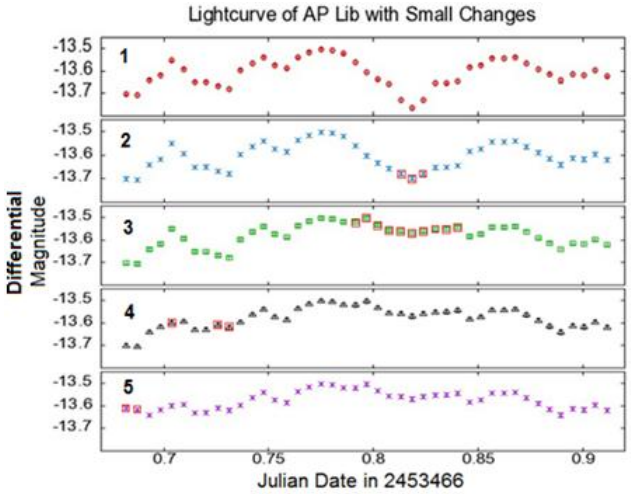

Figure 4.18: *A lightcurve of AP Librae and small changes where the author changed the lightcurve in five steps to remove the flares.*

5 Results

5.1 3c279

Figures 5.1 through 5.10 show lightcurves and SFs of 3c279. The lightcurves of a comparison star are plotted to indicate the significance of the data. The lightcurve of the comparison star in figure 5.3 shows that problems still remain in data reduction. The "flare" seen in this comparison star was seen in all of the comparison stars and was not just a problem with this one comparison star. In order to try to correct this problem, the pixel position versus flux was plotted which showed a trend towards lower flux corresponding to pixels near the edge of the CCD chip. An "illumination correction" may be necessary to fix this. Currently, an illumination correction has not been performed which would be necessary after flatfield corrections, and further work would be needed on this data to do so.

Blazar 3c279 clearly varies from day to day, but no significant microvariability can be seen during the four days of observation. These observations are consistent with observations made by Gupta et al. (2008) in January and February of 2007. The only potential signs of microvariability are coincident with features seen in the comparison stars, which points to data reduction problems.

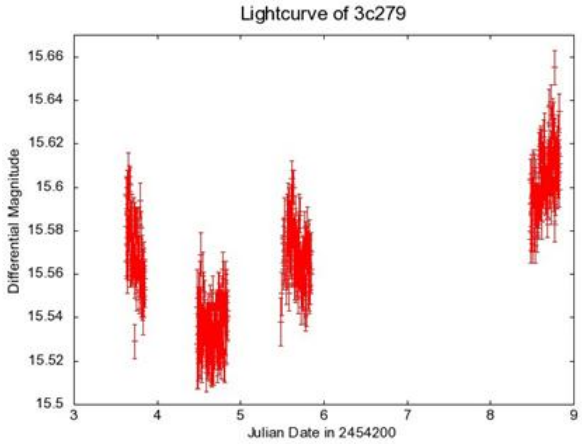

Figure 5.1: *This image shows the lightcurve of 3c279 over the entire observation run.*

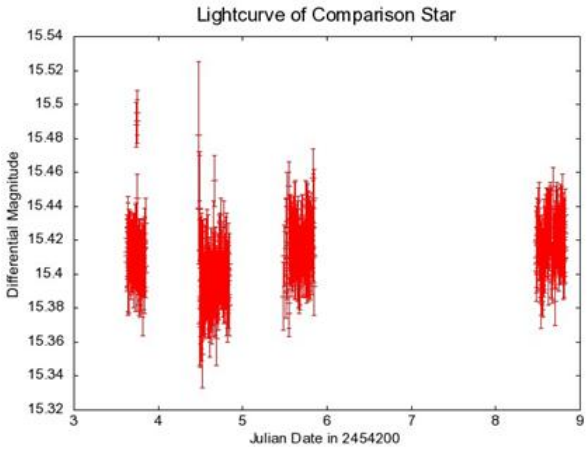

Figure 5.2: *This image shows the lightcurve of a comparison star over the entire observation run.*

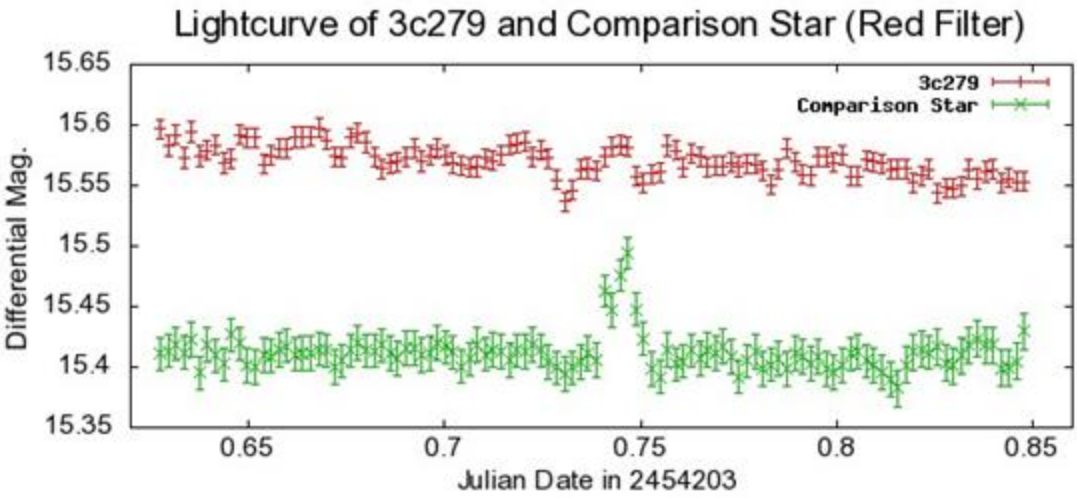

Figure 5.3: *This image shows the lightcurve of 3c279 and a comparison star for night 1. Problems with the data reduction led to the "flare" in the comparison star.*

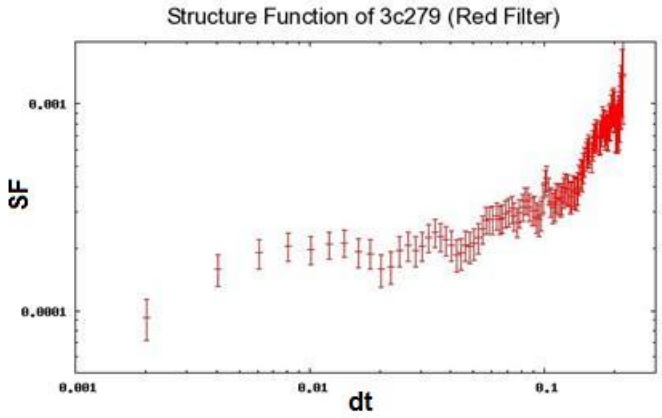

Figure 5.4: *SF of 3c279 on night 1. Due to data reduction problems, a "flare" in the comparison star makes any microvariability not believable. This SF rises to a maximum at the end which is from the 0.5 magnitude downward trend that is seen over the entire night which is believable. This SF is consistent with what Heeschen et al. (1987) call a type I SF with an initial slope between zero and one and no obvious characteristic timescale.*

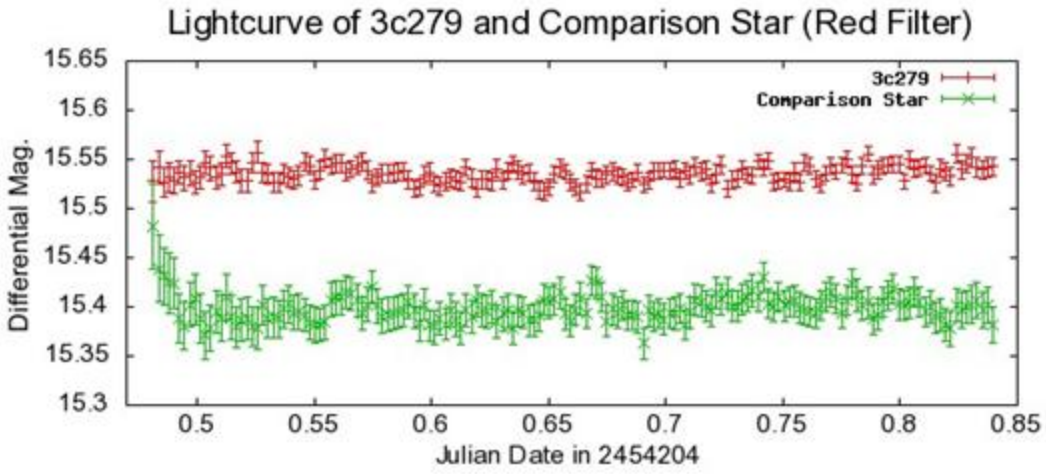

Figure 5.5: *This image shows the lightcurve of 3c279 and a comparison star for night 2.*

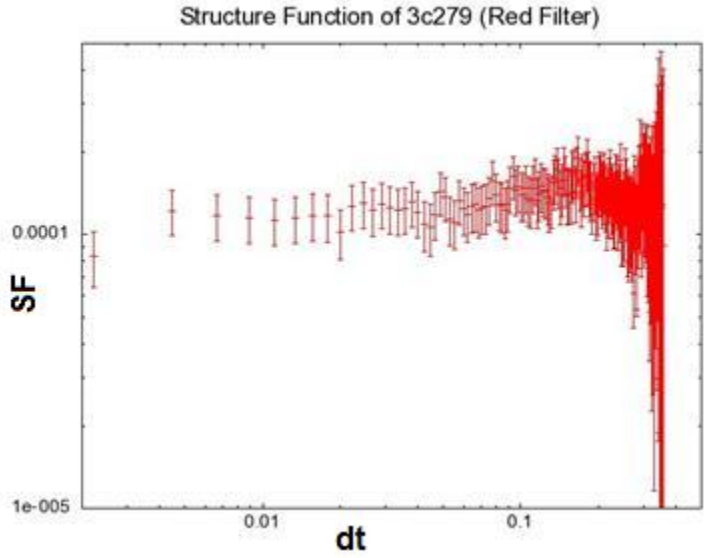

Figure 5.6: *SF of 3c279 on night 2. No microvariability or flicker is detected; the SF resembles the SF that results from white noise.*

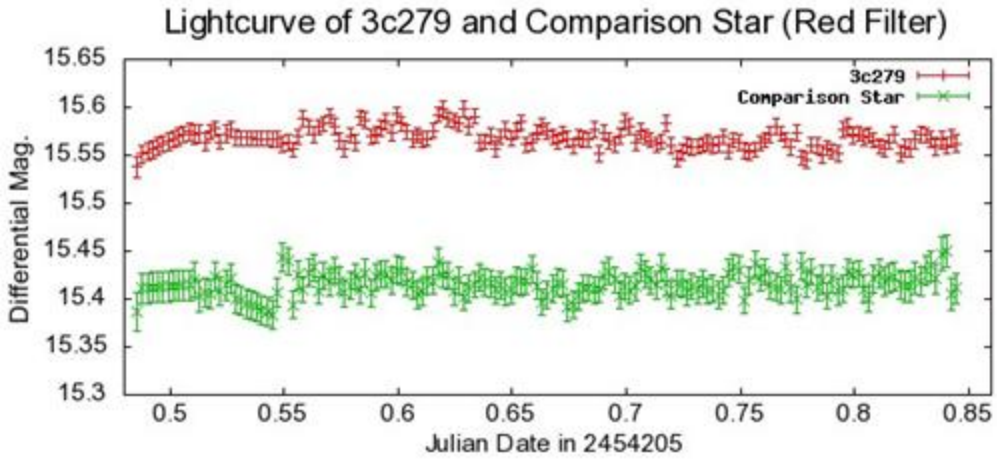

Figure 5.7: *This image shows the lightcurve of 3c279 and a comparison star for night 3.*

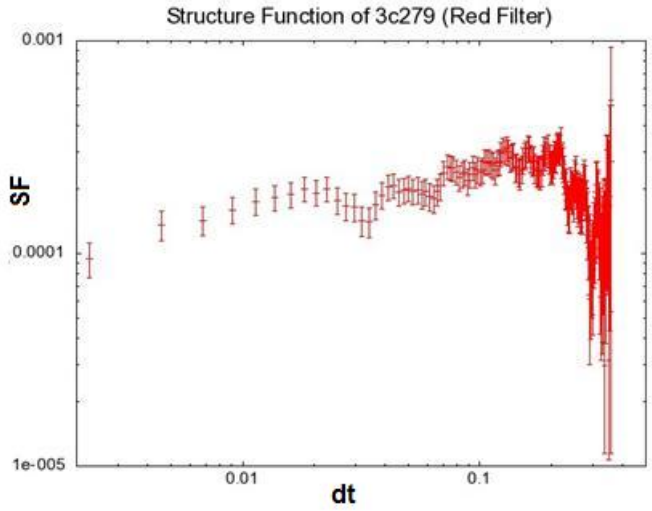

Figure 5.8: *SF of 3c279 on night 3. No microvariability or flicker is detected; the SF resembles fairly closely the SF that results from white noise and there is as much variability in the comparison star as there is in the blazar.*

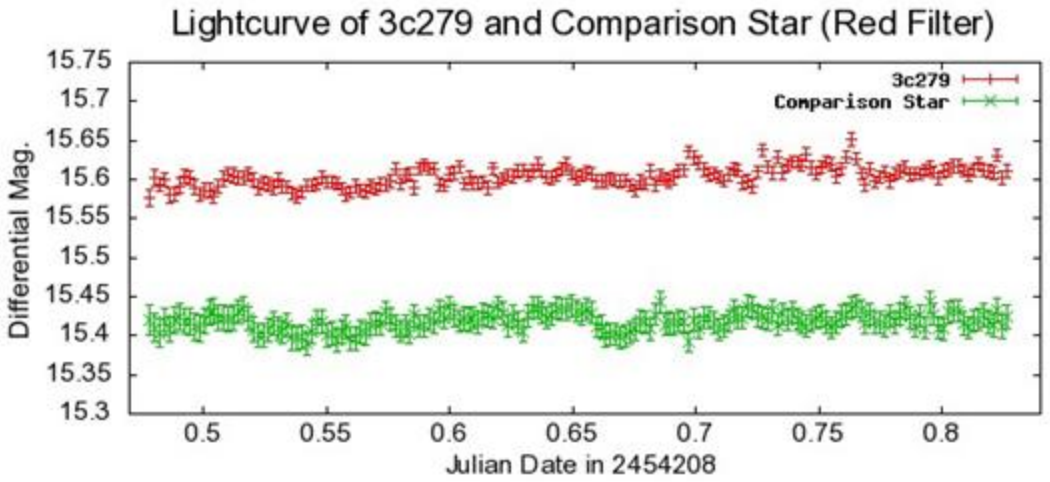

Figure 5.9: *This image shows the lightcurve of 3c279 and a comparison star for night 4.*

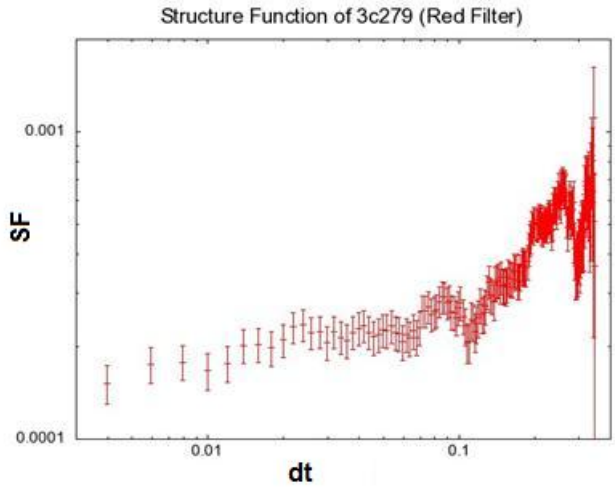

Figure 5.10: *SF of 3c279 on night 4. No microvariability can be believed because the changes in magnitude seen from 3c279 are not bigger than the changes in magnitude seen from the comparison star.*

5.2 AP Librae

Figures 5.11 through 5.16 show the lightcurves and SFs of AP Librae. Microvariability is detected in AP Librae on both nights of observation.

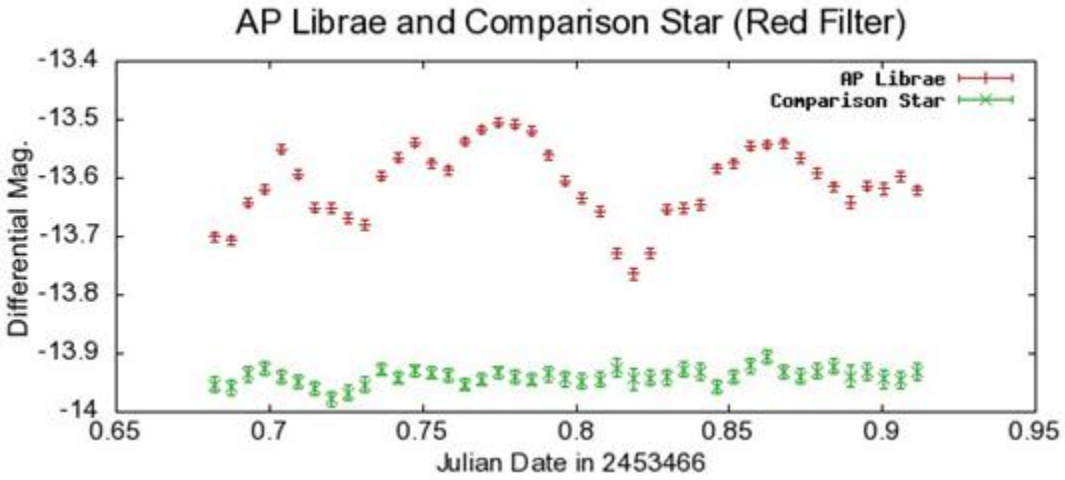

Figure 5.11: *A Lightcurve of AP Librae and a comparison star. The magnitude of the comparison star has a constant added to it so it can be compared with AP Librae.*

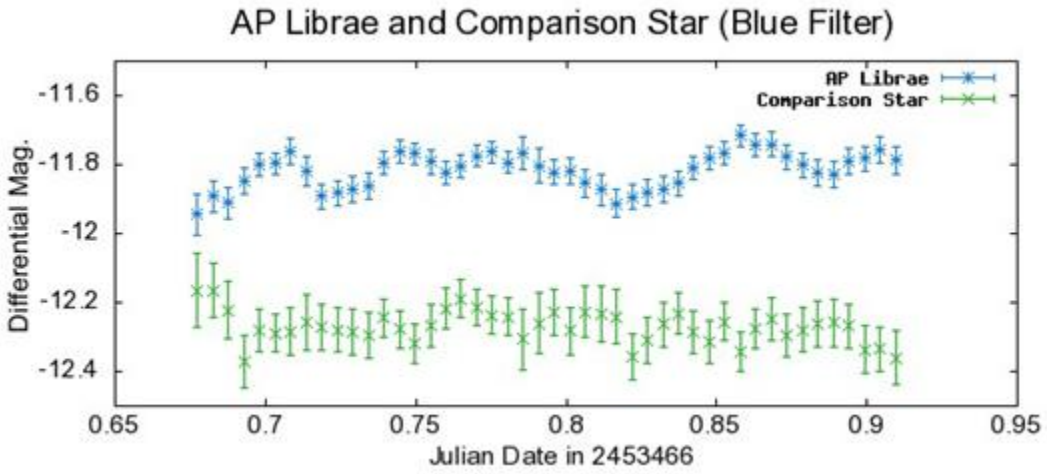

Figure 5.12: *A Lightcurve of AP Librae and a comparison star for night 1. The magnitude of the comparison star has a constant added to it so it can be compared with AP Librae.*

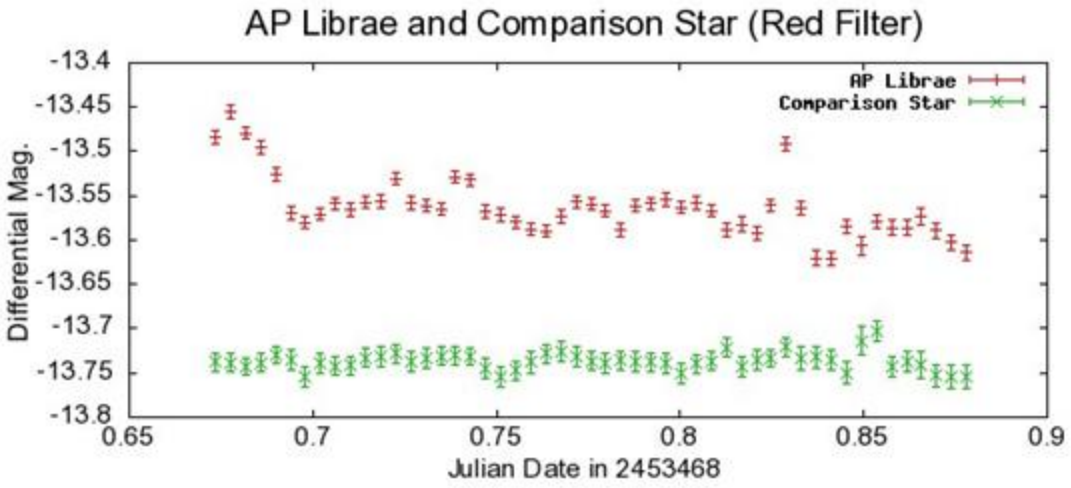

Figure 5.13: *A Lightcurve of AP Librae and a comparison star for night 2. The magnitude of the comparison star has a constant added to it so it can be compared with AP Librae.*

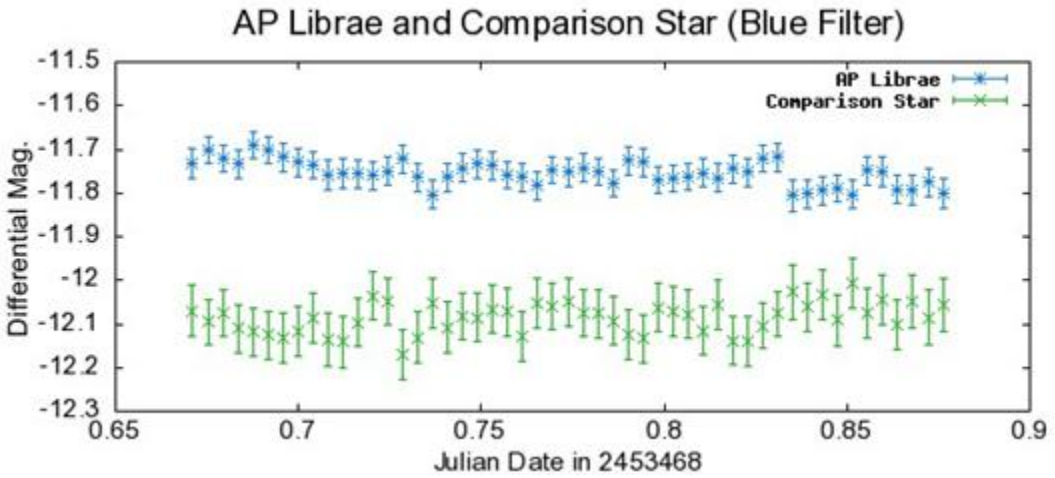

Figure 5.14: *A Lightcurve of AP Librae and a comparison star. The magnitude of the comparison star has a constant added to it so it can be compared with AP Librae.*

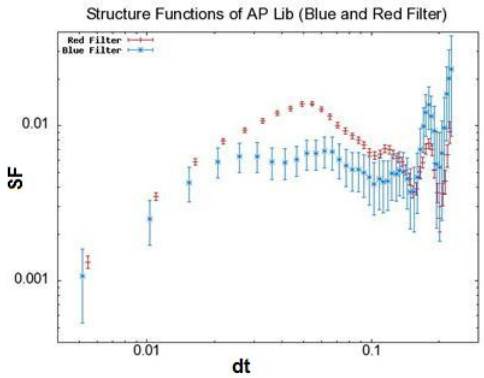

Figure 5.15: *This shows the SFs for AP Librae on JD 2453466. The corresponding lightcurves are shown in figures 5.11 and 5.12. The characteristic timescale for the red filter is about 0.05 JD. In the blue filter however, two characteristic timescales show up. The SF for the R filter resembles what Heeschen et al. (1987) call a type II SF with an initial slope close to one and a characteristic timescale.*

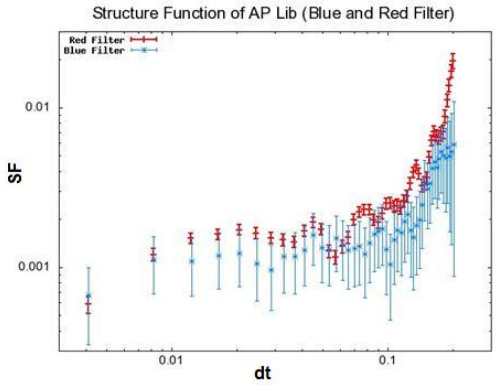

Figure 5.16: *This shows the SFs for AP Librae on JD 2453468. The corresponding lightcurves are shown in figures 5.13 and 5.14. For the blue filter, the error bars suggest no detected characteristic timescale, although the blue and red filter SFs are relatively coordinated. There are two characteristic timescales detected for the red filter SF (0.02 JD and 0.04 JD) which correspond to the two flares seen in the lightcurve where one flare is at the very beginning and the other peaks at a JD of 2453468.83.*

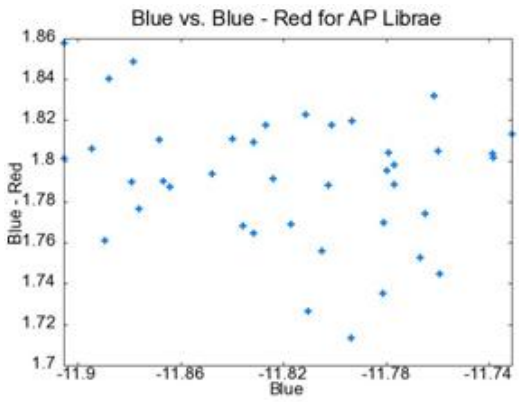

Figure 5.17: *B vs. B minus R plot for AP Librae on night 1.*

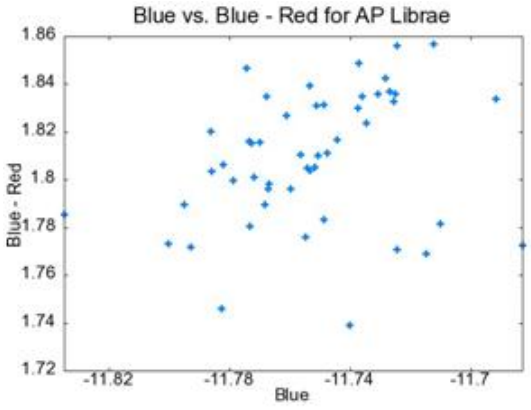

Figure 5.18: *B vs. B minus R plot for AP Librae on night 2.*

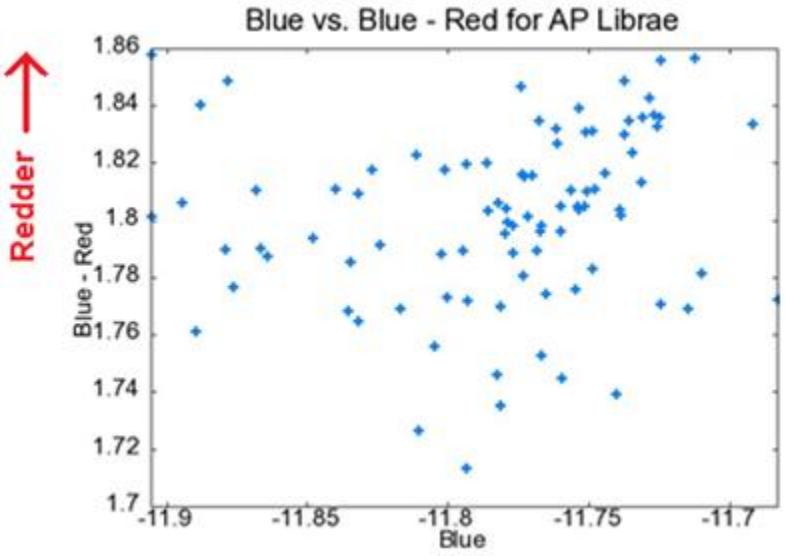

Figure 5.19: *B vs. B minus R for both nights.*

Wagner & Witzel (1995) report that AGNs tend to get bluer when brighter and Stalin et al. (2006) confirm this with their analysis of BL Lacertae. GU et al. (2006) found two AGNs to be redder when brighter, but all the BL Lac objects they looked at were bluer when brighter. AP Librae did not appear to show any correlation between color and brightness on any of the observation nights (see figures 5.17, 5.18 & 5.19).

6 Conclusions

6.1 Microvariability

No microvariability was detected for 3c279 on timescales shorter than a day during any night of observation. Andrew Collazzi already looked at the data for AP Librae in his thesis titled *Microvariability in AP Librae and PKS 1216-010* and saw microvariability which is confirmed by the SF analysis done by the author. AP Librae showed characteristic timescales of variability of as short at 0.02 JD and had a large flare on night one of observation that registered a characteristic timescale of 0.05 JD. For AP Librae there was no correlation found between color and brightness.

6.2 Structure Functions

While SFs pick out characteristic timescales, comparing the lightcurve of the blazars to the comparison star is very important and should not be overlooked because variability from the blazar that is smaller than the largest variability from the comparison star cannot be believed. Overall, SF analysis should be used in close accord with comparison stars and characteristic timescales and periodicity found near the end of a SF should be analyzed properly before confirmed. Also smaller flares in a lightcurve might not show up in a SF if a larger flare is present later in the lightcurve.

6.3 Future Goals

The future of this project should include finishing the data reduction to improve the lightcurves and possibly running different statistical analysis on AP Librae.

7 Acknowledgments & References

Acknowledgments

Dr. Robert Knop
Dr. David James
Dr. David Weintraub
Dr. Thomas Kephart
The Department of Physics and Astronomy at Vanderbilt
My family & friends
Thank you.

References

[1] Blandford, R. D., Narayan, R., Romani, R. W. 1986, ApJ, 301, L53

[2] Collazzi, A., 2006, Vanderbilt Undergraduate Honors Thesis

[3] Ghosh, K.K., Ramsey, B.D., Sadun, A.C., Soundararajaperumal, S., Wang, J., 2000. ApJS 127, 11

[4] Gu M. F., Lee C. U., Pak S., Yim H. S., Fletcher A. B., 2006, A& A, 450, 39

[5] Gupta A. C., Fan J. H., Bai J. M., Wagner S. J., 2008, AJ, 135, 1384

[6] Heeschen D. S., Krichbaum T. P., Schalinski C. J., Witzel A., 1987, AJ, 94, 1493

[7] Hovatta, T., et al. 2007, A& A, 469, 899

[8] Hufnagel, B. R., Bregman, J. N. 1992, ApJ, 386, 473

[9] Krolik, Julian H. *Active Galactic Nuclei.* Princeton, New Jersey: Princeton Universtiy Press, 1999.

[10] Kraus, A., Witzel, A., Krichbaum, T. P. 1999, New Astron. Rev., 43, 685

[11] Meier D. L., Koide S., Uchida Yu., 2001, Sci, 291, 84

[12] Simonetti, J.H., Cordes, J.M., Heeschen, D.S. 1985, ApJ, 296, 46

[13] Stalin C. S., Gopal-Krishna S. R.,Wiita P. J., Mohan V., Pandey A. K., 2006, MNRAS, 366, 1337

[14] Wagner, S.J., Witzel, A., 1995. ARA& A 33, 163

[15] Wiita, P. J. 1996, in Blazar continuum Variability, ed. H. R. Miller, J. R. Webb, J. C. Noble (San Francisco: ASP), ASP Conf. Ser.,110, 42